

## NMR Studies of Lysozyme Surface Accessibility by Using Different Paramagnetic Relaxation Probes

Andrea Bernini,<sup>†,‡</sup> Ottavia Spiga,<sup>†,‡</sup> Vincenzo Venditti,<sup>†</sup> Filippo Prischi,<sup>†</sup> Luisa Bracci,<sup>†</sup>  
Angela Pui-Ling Tong,<sup>§</sup> Wing-Tak Wong,<sup>#</sup> and Neri Niccolai<sup>\*,†,‡</sup>

*Biomolecular Structure Research Center and Dipartimento di Biologia Molecolare, Università di Siena, and SienaBioGrafix Srl, I-53100 Siena, Italy, and SPACE Community College and Department of Chemistry, The University of Kong Kong, Pokfulam Road, HKSAR, China*

Received March 28, 2006; E-mail: niccolai@unisi.it

Soluble paramagnetic probes have been shown to be useful for obtaining insight into processes regulating protein surface accessibility. The absence of specific interactions between proteins and paramagnetic probes is a prerequisite for describing induced perturbation profiles of protein NMR signals in terms of structure and/or dynamics. Since TEMPOL and Gd(III)DTPA–BMA seem to fulfill this requirement, they have been widely used to study the surface accessibility of proteins.<sup>1–6</sup>

Alternative neutral paramagnetic probes with larger molecular size and higher relaxivity are, however, needed to reduce the amount of probe used in NMR experiments and hence its possible interference with the investigated molecular system. A larger molecular size than those of the above probes could be also useful for defining protein aggregation processes, as protein surface accessibility is dependent on protein–protein interactions: the larger the probe, the more it will be excluded from the surface of the approaching protein molecules.<sup>7</sup>

We used a neutral Gd(III) complex with two metal ions coordinated by a large macrocyclic ligand, shown in Figure 1, as a paramagnetic probe to study hen egg white lysozyme (HEWL) surface accessibility. TEMPOL-induced perturbation profiles<sup>5</sup> and aggregation<sup>8</sup> have been investigated in detail in HEWL and this protein seems suitable for testing the characteristics of [Gd<sub>2</sub>(L7)–(H<sub>2</sub>O)<sub>2</sub>].

Experimental conditions ensuring very limited association of HEWL were used,<sup>8</sup> i.e., 1.0 mM protein concentration, pH 4.0, no salts added, and a temperature of 308 K. Paramagnetic attenuations, *A<sub>i</sub>*, of 54 well-resolved CαH signals from <sup>1</sup>H–<sup>13</sup>C HSQC HEWL spectra, obtained in the presence and in the absence of TEMPOL and [Gd<sub>2</sub>(L7)–(H<sub>2</sub>O)<sub>2</sub>], were compared. Figure 2 summarizes the set of paramagnetic attenuations obtained with 33.0 and 0.7 mM TEMPOL and [Gd<sub>2</sub>(L7)–(H<sub>2</sub>O)<sub>2</sub>], henceforth referred to as *A<sub>i</sub>T* and *A<sub>i</sub>Gd<sub>2</sub>*, respectively. Probe concentrations have been carefully chosen to obtain sizable and similar average signal broadenings in preliminary HEWL 1D spectra. Due to possible inaccuracy in peak volume measurements, *A<sub>i</sub>* values have been discussed outside the estimated maximum error of ±0.15. Thus, only *A<sub>i</sub>* differences larger than twice the standard deviation from the difference average in each set of data, σ = 0.29, have been considered. The data reported in Figure 2 (shown also in the Supporting Information) suggest that *A<sub>i</sub>Gd<sub>2</sub>* and *A<sub>i</sub>T* are rather similar, since *A<sub>i</sub>Gd<sub>2</sub>* is significantly larger than *A<sub>i</sub>T* in only eight cases, while the opposite behavior can be observed in three cases. It is interesting to note that the *A<sub>i</sub>Gd<sub>2</sub>* ≫ *A<sub>i</sub>T* condition holds for five glycyl and two seryl residues, both of

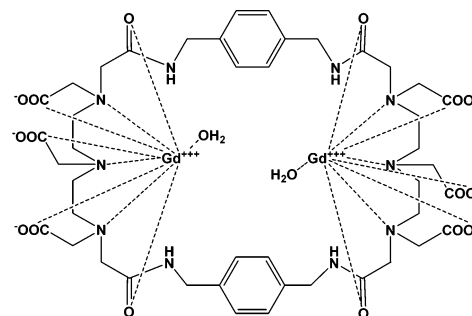


**Figure 1.** Drawing of the structure of [Gd<sub>2</sub>(L7)(H<sub>2</sub>O)<sub>2</sub>], where L7 is 4,7,10,23,26,29-hexakis(carboxymethyl)-2,12,21,31-tetraoxo-1,4,7,10,13-, 20,23,26,29,32-decaazatricyclo[14,20]-*p*-xylene.

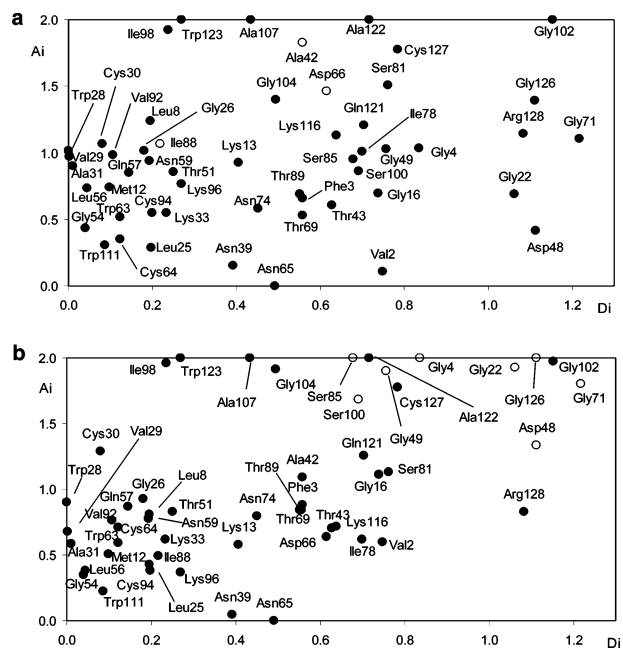


**Figure 2.** Comparison of paramagnetic attenuation (*A<sub>i</sub>*) due to the presence of TEMPOL (a) and [Gd<sub>2</sub>(L7)(H<sub>2</sub>O)<sub>2</sub>] (b) vs residue depth (*D<sub>i</sub>*). Open circles refer to residues whose *A<sub>i</sub>Gd<sub>2</sub>*–*A<sub>i</sub>T* differences are larger than twice the standard deviation from the difference average.

these amino acids being characterized by small side chains. According to the HEWL structure with the Protein Data Bank ID code 193L,<sup>9</sup> all these residues are located in convex surface areas of the protein. The lack of bulky side chains and the particular local shape where they are placed seem to make the latter Gly and Ser backbone methylenes particularly suitable for approach by the large paramagnetic Gd(III) complex. In fact, preferential interac-

<sup>†</sup> Università di Siena.

<sup>‡</sup> SienaBioGrafix Srl.

<sup>§</sup> SPACE Community College.

<sup>#</sup> Department of Chemistry, The University of Kong Kong.

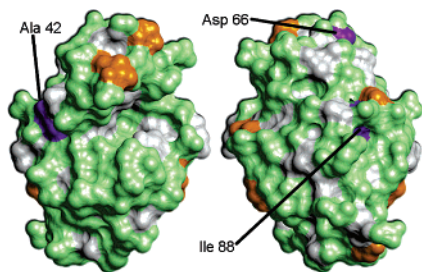


**Figure 3.** Surface representation of HEWL structure, colored according to the similarity observed for  $A_{iGd2}$  and  $A_{iT}$ . Orange patches refer to regions where the condition  $A_{iGd2} \gg A_{iT}$  holds, while the opposite situation is highlighted by purple. Gray patches indicate surface regions where equal paramagnetic effects were induced by the two probes. Surface atoms are colored within a sphere of 3.5 Å radius centered on the considered CαH's.

tions of  $[Gd_2(L7)(H_2O)_2]$  with glycyl and seryl residues can be excluded, as  $A_{iGd2} \leq A_{iT}$  is found for Gly16, Gly26, Gly54, and Ser81.

To investigate how all the observed paramagnetic effects correlate with HEWL structural features,  $A_i$  was expressed in terms of the corresponding atom depths, rather than accessible surface areas, due to the through-space character of the dipolar interaction between nuclear and electronic spins. By inspection of Figure 2, a better correlation between atom depths, expressed as depth index  $D_i$ ,<sup>10</sup> and  $A_i$  obtained in the presence of the Gd complex is apparent. Methyne hydrogens having  $D_i$  higher than 0.6, i.e., hydrogens close to the protein surface, exhibited high or intermediate  $A_{iGd2}$  values and, in contrast, CαH's located near the protein core with  $D_i$  values lower than 0.5 have  $A_{iGd2} < 1.0$ . The anomalously high  $A_{iGd2}$  values observed for Ala107, Ile98, and Trp123 signals, confirmed also by TEMPOL-induced attenuations, support their location in surface hot spots, in line with previous observation in HEWL<sup>5</sup> and in other protein systems using TEMPOL.<sup>11</sup>

It should be noted that, by using the above-mentioned method of calculating atom depths, surface convexity yields reduced atom depths, i.e., higher  $D_i$  values. At the molecular level, surface convexity is more favorable for close approaches of large molecular probes. The fact that the molecular volumes of  $[Gd_2(L7)(H_2O)_2]$  and TEMPOL are very different (1084 and 200 Å<sup>3</sup> respectively have been calculated with the MolMol software package<sup>12</sup>) partially accounts for the good agreement between the obtained HEWL  $A_{iGd2}$  and the calculated  $D_i$  values of the protein methynes.

The fact that  $A_{iT} \gg A_{iGd2}$  is obtained for Ala42, Asp66, and Ile88 may be attributed to two different reasons: in the case of these Ala and Ile residues, it is apparent that they are both located in concave surface regions (see Figure 3), less approachable by the larger probe. The origin of the high  $A_{iT}$  value of Asp66, located in a rather flat part of the HEWL surface, may be ascribed, instead, to some hydrogen bonding of hydroxyl and/or N-oxy moiety of TEMPOL with nearby protein donor groups. The same mechanism could contribute also to the anomalous  $A_{iT}$  value of Ala42, as the HEWL reference structure used indicates that both Asp66 and Ala42 CαH groups are close to surface-exposed hydrogen-bonding donors, i.e., Asp66 and Thr43 backbone amide hydrogens, respectively, which are not involved in any intramolecular hydrogen bonding. Hence, the lifetime of TEMPOL close contacts with the HEWL

surface may be longer in the two regions where Asp66 and Ala42 are located, yielding stronger paramagnetic effects. Due to the critical role of Asp66 in HEWL amyloidosis<sup>13</sup> and, in general, of surface-exposed backbone amides in conformational disorders,<sup>14</sup> a new interesting application of  $A_{iT}$  for delineating potential protein aggregation sites may be suggested.

From Figure 2, a disagreement between the surface proximity of Asn39 and Asn65 methynes and the corresponding paramagnetic perturbations is apparent. The presence of structured water molecules, preventing a close approach of both probes toward these CαH's, is fully supported by our previous HEWL hydration study.<sup>5</sup> In fact, for both Asn39Hα and Asn65Hα, water–protein nuclear Overhauser effects could be detected, indicating their involvement in the formation of strong surface hydration sites (see Supporting Information).

Thus, the reported combined analysis of the paramagnetic effects on <sup>1</sup>H–<sup>13</sup>C HSQC signals due to the presence of TEMPOL and  $[Gd_2(L7)(H_2O)_2]$  seems to confirm that the new probe is very suitable to map protein surface accessibility, as no preferential interaction could be monitored for it. Furthermore, the present data and analyses suggest that a combined use of paramagnetic probes of different size and chemical nature may reveal fine aspects of the complex dynamics occurring at the water–protein interface.

**Acknowledgment.** Thanks are due to the University of Siena for financial support. W.-T.W. thanks the Hong Kong Research Grants Council (HKU7116/02P) and the University of Hong Kong for financial support. A.P.-L.T. thanks The University of Hong Kong for financial support.

**Supporting Information Available:** Complete list of HEWL hydrogens showing water–protein Overhauser effects together with details of the synthesis of  $[Gd_2(L7)(H_2O)_2]$  and of  $A_i$  and  $D_i$  calculations. This material is available free of charge via the Internet at <http://pubs.acs.org>.

## References

- Petros, A. M.; Neri, P.; Fesik, S. W. *J. Biomol. NMR* **1992**, *2*, 11–18.
- Niccolai, N.; Ciutti, A.; Spiga, O.; Scarselli, M.; Bernini, A.; Bracci, L.; Di Maro, D.; Dalvit, C.; Molinari, H.; Esposito, G. T.; Temussi, P. *J. Biol. Chem.* **2001**, *276*, 42455–42461.
- Pintacuda, G.; Otting, G. *J. Am. Chem. Soc.* **2002**, *124*, 372–373.
- Niccolai, N.; Spadaccini, R.; Scarselli, M.; Bernini, A.; Crescenzi, O.; Spiga, O.; Ciutti, A.; Di Maro, D.; Bracci, L.; Dalvit, C.; Temussi, P. *Protein Sci.* **2001**, *10*, 1498–1507.
- Niccolai, N.; Spiga, O.; Bernini, A.; Scarselli, M.; Ciutti, A.; Fiaschi, I.; Chiellini, S.; Molinari, H.; Temussi, P. *J. Mol. Biol.* **2003**, *332*, 437447.
- Liepinsh, E.; Baryshev, M.; Sharipo, A.; Ingelman-Sundberg, M.; Otting, G.; Mkrtchian, S. *Structure* **2001**, *9*, 457–471.
- Bernini, A.; Spiga, O.; Ciutti, A.; Venditti, V.; Prisch, F.; Governatori, M.; Bracci, L.; Lelli, B.; Pileri, S.; Botta, M.; Barge, A.; Laschi, F.; Niccolai, N. *Biochim. Biophys. Acta* **2006**, *1764*, 856–862.
- Gottschalk, M.; Halle, B. *J. Phys. Chem. B* **2003**, *107*, 7914–7922.
- Barman, H. B.; Westbrook, G.; Bhat, T. N.; Weissing, H.; Shindyalov, I. N.; Bourne, P. E. *Nucleic Acids Res.* **2000**, *28*, 235–242.
- Varrazzo, D.; Bernini, A.; Spiga, O.; Ciutti, A.; Chiellini, S.; Venditti, V.; Bracci, L.; Niccolai, N. *Bioinformatics* **2005**, *21*, 2856–2860.
- Scarselli, M.; Bernini, A.; Segoni, C.; Molinari, H.; Esposito, G.; Lesk, A. M.; Laschi, F.; Temussi, P.; Niccolai, N. *J. Biomol. NMR* **1999**, *15*, 125–133.
- Koradi, R.; Billeter, M.; Wüthrich, K. *J. Mol. Graphics* **1996**, *14*, 51–55.
- Frare, E.; Polverino de Lauro, P.; Zurdo, J.; Dobson, C. M.; Fontana, A. *J. Mol. Biol.* **2004**, *340*, 1153–1165.
- De Simone, A.; Dodson, G. G.; Verma, C. S.; Zagari, A.; Frateranali, F. *Proc. Natl. Acad. Sci. U.S.A.* **2005**, *102*, 7535–7540.

JA062109Y